JOURNAL OF AIRCRAFT
Vol. 42, No. 5, September–October 2005

Flow on the Apex of a Sharp-Edged Delta Wing

Niek G. Verhaagen* and Victor F. Kunst†
Delft University of Technology, 2600 GB Delft, The Netherlands

This paper describes a study of the topology of the skin-friction line pattern on a sharp-edged 65-deg swept delta wing. Special attention is paid to the flow pattern on the apex. Because the pattern on this part of the wing is poorly resolved in experiments, a large-scale model of the apex was constructed to obtain more insight into the flow topology. The angle of attack is shown to have a strong effect on the apex flow topology. The topology shows evidence of primary and secondary separation.

Introduction

DELTA-WING planforms are used for many current fighter aircraft and in designs of future fighter and UCAV configurations. Such aircraft rely on lift generated by vortex flow to enhance maneuverability. Strong leading-edge vortices generated along the leading edge of the highly swept delta wings have a dominant effect on the flow and air loads. At high angle of attack, a sudden disorganization of the structure of the leading-edge vortex core flow occurs, known as vortex breakdown. The disorganized core flow induces strong fluctuations of the wing surface pressures downstream of the vortex breakdown point. Interaction with tail surfaces results in so-called tail buffeting. The consequences of these phenomena are a deterioration of aircraft performance, stability, and control. Mitchell et al.[1] have recently given an overview of experimental databases on vortex core breakdown and of state-of-the-art numerical solutions.

The present study is part of a research program that was conducted at the Delft University of Technology (TUD) to investigate the causes of the strong nonlinearities (critical states) occurring in the forces and moments of a 65-deg delta wing at sideslip.[2] The authors used flow visualization data to determine the effects of sideslip on the topology of the surface flow in an effort to explain the behavior of the surface pressures with sideslip. Difficulties were encountered in inferring the topology of the flow at the apex due to poor resolution of the streakline pattern. The apex region is of interest because the vortices on the delta wing can be expected to originate there.

The present study pays attention to the flow at the apex. At this stage only the flow at zero sideslip is considered. For this condition, several theoreticians[3–6] have postulated the topology of the flow at the apex of a sharp-edged delta wing wherein the apex is considered on a microscopic scale. Because few experimental data exist to verify their postulates, a scale model of the apex was constructed to improve the resolution of the apex flow. Preliminary tests conducted on this so-called apex model showed a complex skin-friction line pattern to exist at $\alpha = 30$ deg.[7] To better understand the formation of this pattern, in the present study the flow on the apex model has been visualized at α between 0 and 30 deg.

In this paper, a study of flow on the original 65-deg delta wing is first described. The skin-friction line pattern is analyzed qualitatively using topology theory. A brief description of this theory is given. Subsequently, attention is paid to the topology of the flow on the apex model and to existing theoretical postulates. Finally, the results of the visualization study carried out on the apex model are described.

Delta-Wing Experiment

Flow visualization tests were conducted on a model of a flat-plate 65-deg swept delta wing. Dimensions are shown in Fig. 1. The wing has a constant thickness of 20 mm, yielding a thickness-to-chord ratio t/c of 0.03. The leading and trailing edges are "sharp" (radius 0.1 mm) and beveled on only the lower (windward) surface at 31 and 23 deg, respectively.

The wing was tested in the low-turbulence tunnel of the TUD Department of Aerospace Engineering. This is a closed-circuit tunnel with an octagonal solid-wall test section 1.80 m wide, 1.25 m high, and 2.60 m long. The tests were conducted at a constant $\alpha = 30$ deg and at an airspeed of 50 m/s, yielding a Mach number M of 0.15. The chord Reynolds number equals 2.3×10^6.

Flow visualization tests indicated that the cores of both the left and right leading-edge vortices break down at the 20% root chord station ($x/c = 0.20$). The high airspeed and large angle of attack generated very low pressures and temperatures in the cores of the leading-edge vortices. Consequently, natural condensation of the flow occurred in the cores. The vortex cores and breakdown location could be observed with the naked eye. The vortex breakdown point was defined to be located at the point where the core started to diffuse. This point was observed to oscillate at a frequency of 4–5 Hz. The amplitude of the oscillations was about 3% of the root chord length.

Flow on the wing was visualized using two different fluids. One fluid, called oil-flow fluid, consisted of a mixture of titanium dioxide, pipe clay, a surface tension relaxant, and kerosene. The other fluid was a mixture of fluorescent dye and oil. The latter mixture was visualized using ultraviolet light. Figure 2 shows the leeward-surface pattern visualized with the oil-flow and fluorescent fluids. The fluorescent fluid has the advantage over the oil-flow fluid that it does not dry while the tunnel is running, making it possible to observe changes to the surface pattern with time. The fluid resolved the location of the secondary-separation lines very well, but outboard of these lines the resolution was low compared to that of the pattern visualized with the oil flow. The flow patterns were recorded on still photographs and digital video.

Topology Theory

The observed streakline patterns were analyzed using topology theory.[4,6,8] This theory qualitatively describes the pattern formed by the streaklines and assumes that the pattern can be used to determine a time-averaged phase portrait of the surface flow that consists of a continuous vector field with a limited number of singular points. The singular points occur at isolated points where the skin-friction vector becomes identically zero. In a two-dimensional field the phase portraits can be classified in terms of the trace ($p = \lambda_1 + \lambda_2$) and determinant ($q = \lambda_1 \cdot \lambda_2$) of the Jacobian matrix of the skin-friction line partial derivatives. As shown in Fig. 3, depending on the value of (p, q), phase portraits can be classified as saddles, nodes, and foci, and also as centers, star-shaped sinks, and sources. Through a saddle S pass only two skin-friction lines, whereas all the other

Presented as Paper 2004-1065 at the AIAA 42nd Aerospace Sciences Meeting and Exhibit, Reno, NV, 5–8 January 2004; received 19 April 2004; revision received 30 March 2005; accepted for publication 31 March 2005.

*Research Scientist, Department of Aerospace Engineering. Member AIAA.
†Former Thesis Student, Department of Aerospace Engineering.

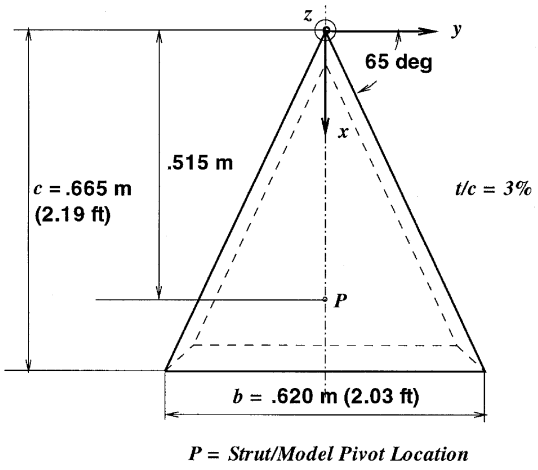

Fig. 1 TUD wing geometry.

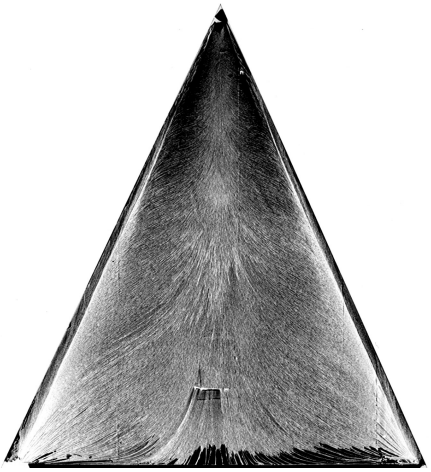

a)

b)

Fig. 2 Leeward-surface flow pattern visualized using different visualization fluids: a) oil-flow and b) fluorescent-dye/oil.

lines miss the origin and take directions consistent with those of the adjacent lines. Nodes can be subdivided into nodal points and foci. At a nodal point there is one tangent line. All skin-friction lines are directed either outward away from the node (a nodal point of attachment N_a) or inward toward the node (a nodal point of separation N_s). The other type of node, the focus N_f, has no common tangent line. All skin-friction lines spiral around the origin, either out of it (a focus of attachment) or into it (a focus of separation). It should

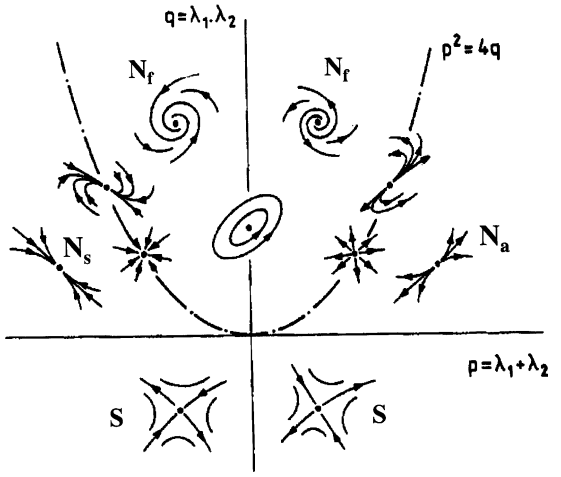

Fig. 3 Classification of phase portraits in (p, q) plane (Bakker[8]).

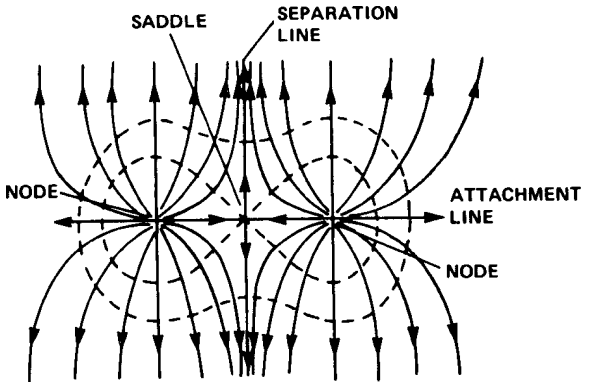

Fig. 4 Nodes and saddle point combination (Lighthill[3]).

be noted that the qualitative properties of the vector field are determined if the location and the type of singular points are known. The number and the combination of singular points on a wing or body must obey certain rules. These are discussed in Refs. 3, 9, and 10.

Three-dimensional flow separation occurs when skin-friction lines emerging from nodes are converging onto a so-called line of separation and a separation surface stems from this line. This is illustrated in Fig. 4. The converse of a separation line is a line of attachment. The skin-friction lines tend to diverge from such a line.

Flow on Delta Wing

Figure 5 shows the topology of the skin-friction line pattern on the windward and leeward surfaces of the delta wing. Short dashed lines mark the inboard boundary of the beveled edges on the windward surface. The transition from the beveled edges to the flat lower surface is sharp, not rounded. For reference, the inside corners of the transition lines are marked A, B, and C. A long dash-dot line marks the centerline of the wing. Solid lines (or curves) indicate surface skin-friction lines. Separation and attachment lines are marked S_i and A_i, respectively, where subscript i is a sequence number.

On the windward surface, an attachment line A_0 is visible at the nose centerline (see insert Fig. 5a). The free flow impinges at the stagnation point just downstream of the apex. In the topology the stagnation point is a node of attachment N_a, the origin of all skin-friction lines wrapping the wing. Downstream of the nose, the attachment line A_0 splits into two separate lines that terminate at the wing tips. Outboard of these lines, the shear flow bends toward the leading edge and leaves the wing at the primary-separation line S_1. Inboard of the two attachment lines A_0, the skin-friction lines are parallel to the wing centerline and directed toward the trailing edge. At the wing tips a series of small-scale vortical structures have been observed.[2] As a result of these tiny vortices, the flow topology in these regions may contain multiple small-scale node-saddle combinations. The resolution of the latter singularities is poor and no

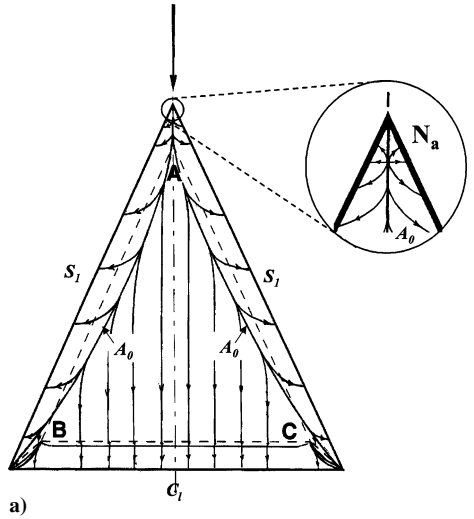

a)

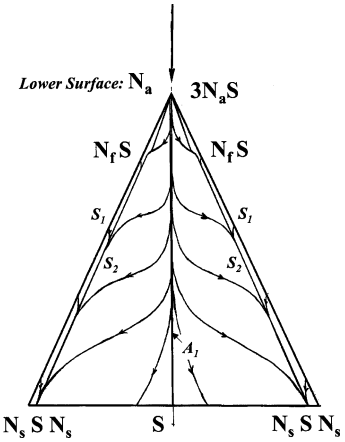

b)

Fig. 5 Topology of skin-friction line pattern: a) windward surface and b) leeward surface.

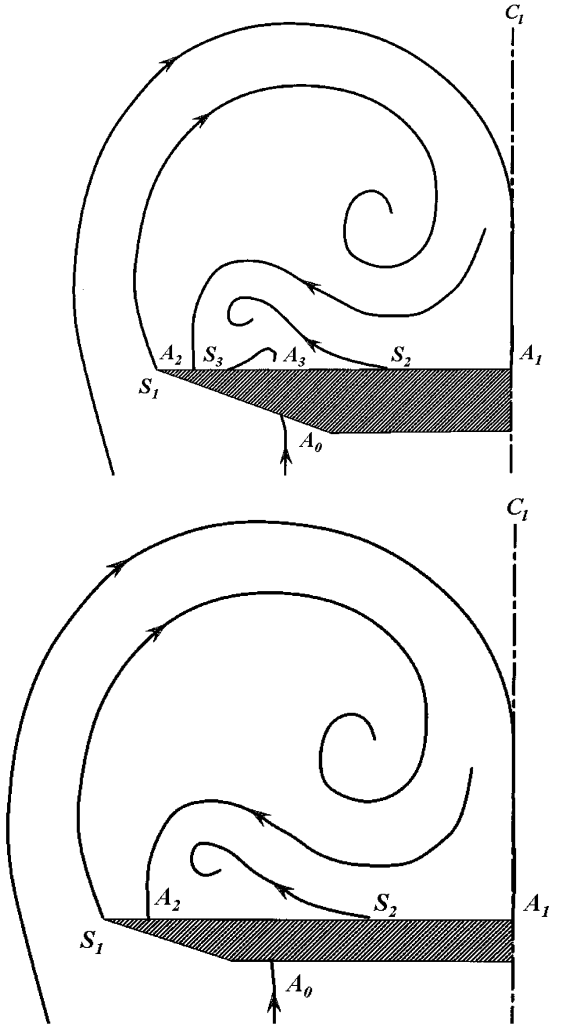

Fig. 6 Vortex cross flow topology upstream (upper plot) and downstream (lower plot) of boundary-layer transition region.

attempt has been made here to infer the topology of the flow on the windward-surface tips.

Figure 5b shows the topology of the skin-friction line pattern on the leeward surface. The separation surface stemming from separation line S_1 rolls up into a primary vortex, which attaches at A_1 on the wing centerline. Integral-shaped curves mark the outward directed skin-friction lines that separate at secondary-separation lines S_2 just inboard of the leading edge. At the apex, a triple node–saddle combination N_aS is suggested. This will be motivated in the next section. At $x/c \approx 0.16$, a kink in S_2 marks the transition of the boundary layer from laminar to turbulent. In the topology an N_fS combination is conjectured in this region. The topology of the vortex crossflow upstream and downstream of this region is sketched in Fig. 6. The primary, secondary, and tertiary separation lines are marked S_1, S_2, and S_3, respectively, the attachment line on the windward surface is denoted A_0, and A_1, A_2, and A_3 are the lines on the leeward surface. The topology of the vortex crossflow downstream of the transition region is well known from experiments and numerical computations.[1] Upstream of the transition region the flow pattern on the delta wing suggests that tertiary separation occurs. This type of separation has also been observed in other experiments.[11,12] Figure 7 shows the conjectured topology of the skin-friction line pattern in this region.

At the wing trailing edge, the flow patterns suggest the existence of a saddle S at the center and an N_sSN_s combination at both tips. For a more detailed description of the singularities at the wing trailing edge, see Ref. 2.

Flow at Apex

This section focuses on the origin of the vortices over the original delta wing, which can be expected to be located somewhere on

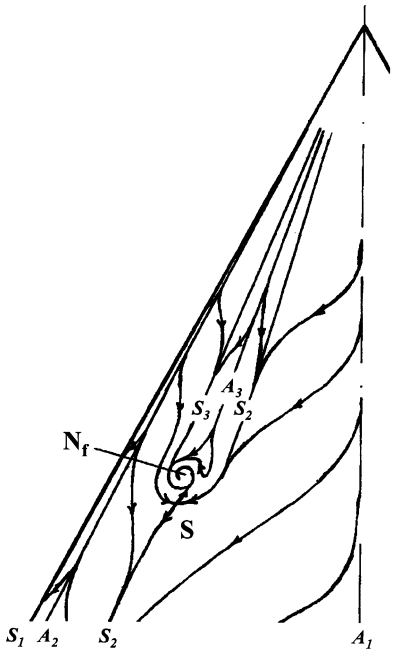

Fig. 7 Conjectured topology of flow at transition region.

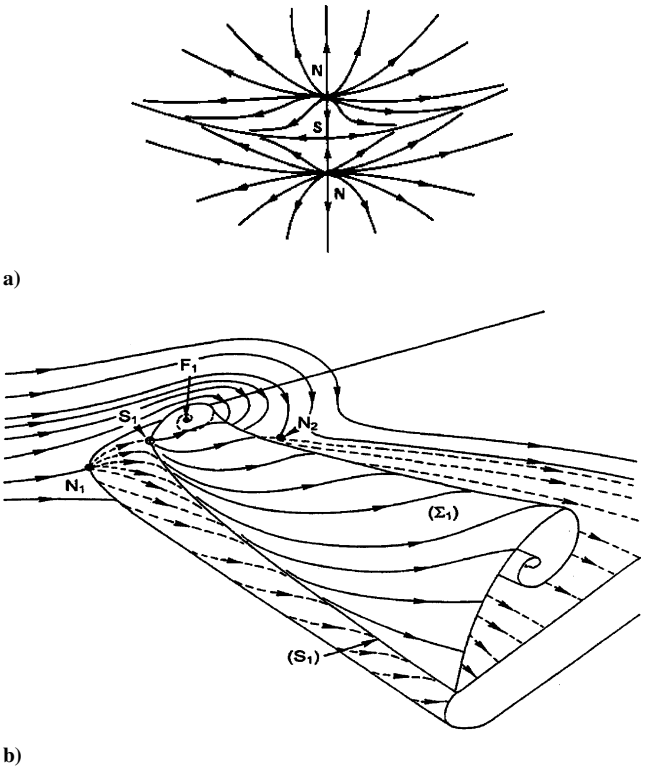

Fig. 8 Theoretical topology of flow at apex: a) postulate by Lighthill[3] and b) development of outer flow, according to Délery.[4]

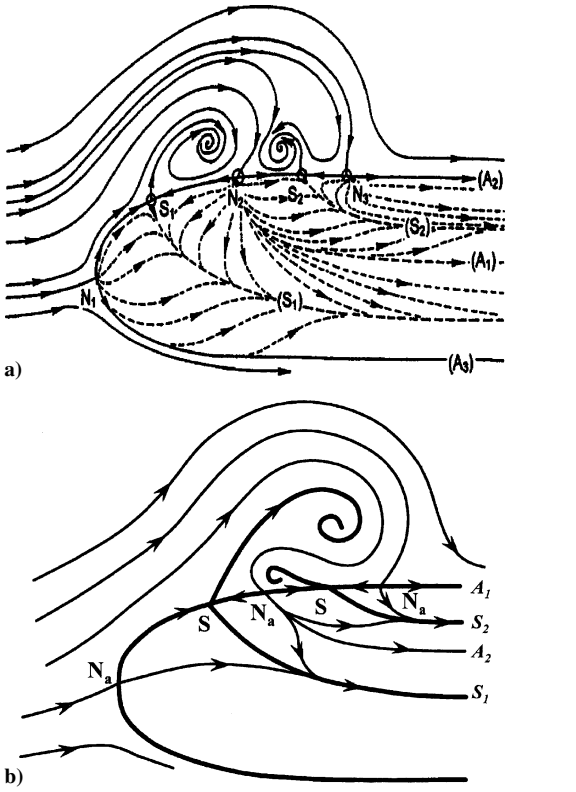

Fig. 9 Two-vortex flow system on apex: a) as conjectured by Délery[4] and b) as postulated here.

the apex. Several theoreticians[3–6] have made conjectures as to the topology of the skin-friction line pattern on the apex. In their theories, the apex is magnified to such an extent that the nose becomes blunt and the edges round.

Lighthill[3] postulates the topology shown in Fig. 8a. It consists of a saddle at the nose and a node of attachment on both the windward and the leeward surface. Figure 8b, from Délery,[4] shows how a primary vortex may evolve from this topology. The separation surface forming this vortex stems from the primary-separation line that originates at the saddle. Because of the shape of the primary vortex over the apex, this is called a U or horseshoe type of separation. Délery also suggests a topology for the crossflow in the xz-plane on the centerline for the case in which a secondary vortex exists. This topology is shown in Fig. 9a. The secondary vortex adds another node–saddle to the singular points on the centerline. The secondary vortex is conjectured to be slightly smaller than the primary vortex and located outboard of this vortex. Figure 9b shows a crossflow that correlates with the topology of the flow further downstream on the delta wing; the secondary vortex is smaller and located below the primary vortex. Note that the topology of the crossflow is equivalent for both cases since they can be deduced from each other by a continuous deformation.

On the apex of the delta wing a triple N_aS combination was conjectured (Fig. 5b). The reason for this is that tertiary separation is believed to add another node–saddle to the twin N_aS combination on the centerline that is associated with primary and secondary separation. The existence of a triple N_aS combination could not be verified on the original delta wing apex because this region is too small to clearly resolve the skin-friction line pattern there.

Figure 10a shows a topology for the flow at the apex postulated by Legendre.[5] The outer flow development is shown in Fig. 10b. In contradiction to the topology suggested by Lighthill, the vortex core now originates from a focus on the wing surface. This type of separation is called a horn type of separation.

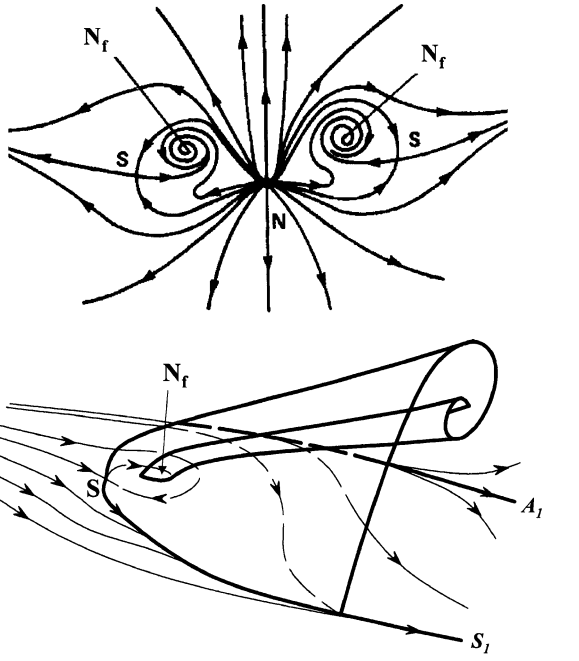

Fig. 10 Theoretical topology of flow at apex: a) postulate by Legendre[5] and b) outer flow development.

Apex Model Experiment

Upstream of bevel corner point A (see Fig. 5a), the delta-wing cross section is an inverted triangle with sharp edges. Close to the apex, on a microscopic scale, the nose is blunt and the edges of a finite radius. This region is the subject of the present study. A wind-tunnel model representing this region is shown in Fig. 11. It has a triangular cross section and rounded edges. Leading edge and nose radii are 20 mm, whereas the length of the model is 187 mm. In comparison to the original delta-wing model, the leading-edge radius of the apex model is 200 times larger. The leading edge sweep of the latter model is identical to that of the delta wing (65 deg). The trailing edge is truncated. The apex model was constructed of PVC material and sprayed black for high contrast with the visualization fluids.

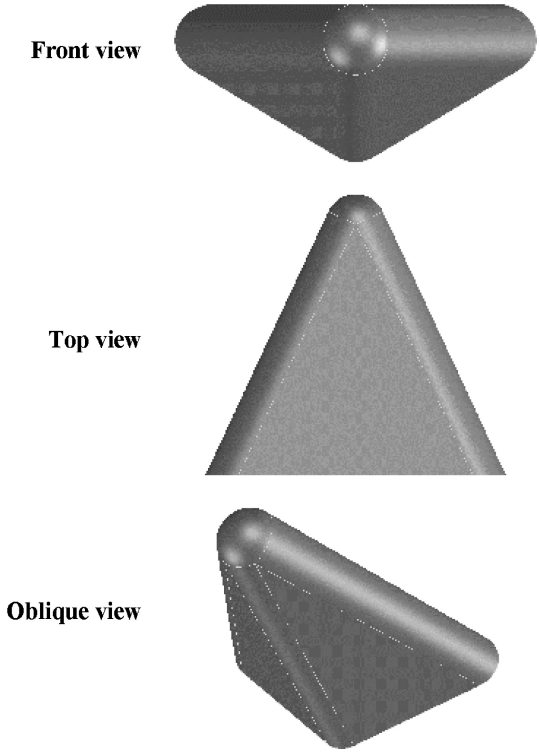

Fig. 11 Apex Model.

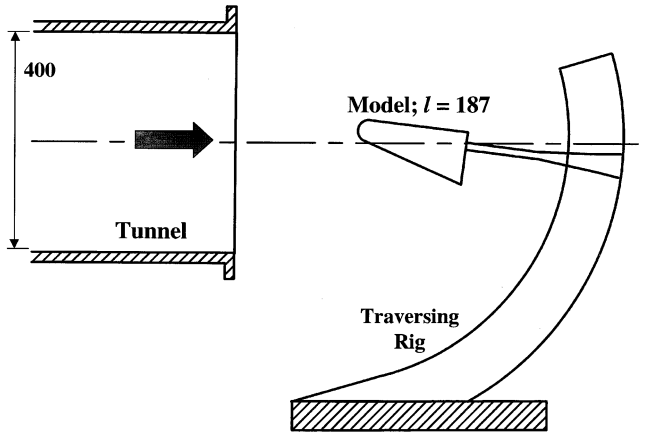

(dimensions in mm)

Fig. 12 Experimental setup.

For visualization the same two fluids were used as before on the original delta wing. The tests were performed in an open low-speed wind tunnel with a nozzle 0.40 m wide and 0.40 m high. An advantage of an open test section is that the visualization fluid can be applied to the model after the air has reached the desired speed. A closed test section has to be opened first and the visualization fluid applied at zero air speed. It then takes some time to close the test section and bring the air to full speed. During this transition time, part of the visualization fluid may dry, resulting in a streakline pattern not corresponding to that generated when the fluid is applied at full speed. The latter is a problem with models whose surface flow is sensitive to Reynolds number effects. Figure 12 shows a schematic of the test setup. The model is mounted on a sting that is fixed to a (α, β) traversing mechanism. The maximum α that can be reached with this mechanism is 30 deg. The visualization tests have been conducted at an air speed of 20 m/s.

Preliminary tests conducted at $\alpha = 30$ deg showed a complex flow pattern.[7] To better understand how this pattern is formed, we

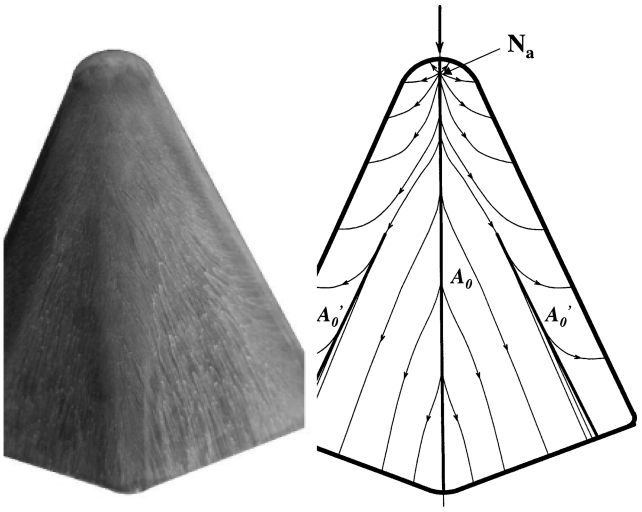

Fig. 13 Flow on windward surface at $\alpha = 20$ deg.

investigated the flow pattern at α from zero and 30 deg. The flow patterns were recorded on photographic film and digital videotape. The photographs were used to draw the skin-friction line patterns. The video images showed the direction of the shear flow and were used to determine the location and the type of the singularities.

Flow on Apex Model

Figure 13 shows a photograph of the oil-flow pattern and a schematic of the conjectured topology of the flow pattern on the windward surface of the apex model at $\alpha = 20$ deg. Over the range of α tested here, the flow topology was observed not to change with α. At zero α the stagnation point is located on the nose. This point moves a short distance downstream from the nose with increasing α. A node N_a is located at the stagnation point. An attachment line A_0 emanates downstream from this node. Another attachment line A_0' exists closer to the leading edge. Outboard of this line, the skin-friction lines sweep around the round leading edge and separate at the primary-separation line S_1.

Figure 14 shows the oil-flow pattern and the topology of the skin-friction line pattern on the leeward surface for $\alpha = 0$, 20, and 30 deg. On the body, the footprint of the primary and secondary vortices can be noted. The integral-shaped curves mark the direction of the shear flow induced by these vortices. The width of the footprints increases with α due to an increase in vortex size. At $\alpha = 30$ deg, on the rear part of the model a kink in S_2 can be noted. Upstream effects of the truncated trailing edge may cause this.

The behavior of the boundary layer was investigated using a microphone. The boundary layer was noted to be laminar on the windward and leeward surfaces up to the separation lines S_1, whereas inboard of these lines the flow is turbulent. This holds for all α tested here.

The conjectured topology of the flow on the nose–body junction is shown in detail in Fig. 15. At zero α, a complex topology characterized by an oval footprint is observed. Inside the footprint a pair of counterrotating foci N_f are observed. Primary-separation line S_1 emanates from the most upstream saddle S and proceeds through a more outboard located saddle in downstream direction. On the bottom of the footprint, three nodes N_a and two saddles are conjectured. Secondary-separation line S_2 is conjectured to originate from a focus N_f. The direction of rotation of the separation surface forming the secondary vortex correlates with the sense of rotation of the focus. It is unclear how the primary separation occurs. The separation surface emanating from S_1 may evolve overhead the secondary vortex Separation lines S_1 and S_2 can be seen to proceed all the away to the trailing edge. The flow pattern suggests that a primary and a secondary vortex exists on each model half. These vortices occur over the model, unless the fact that the upper surface is parallel to the direction of the free stream. The reason for this is the positive camber of the model, which induces an effective upflow.

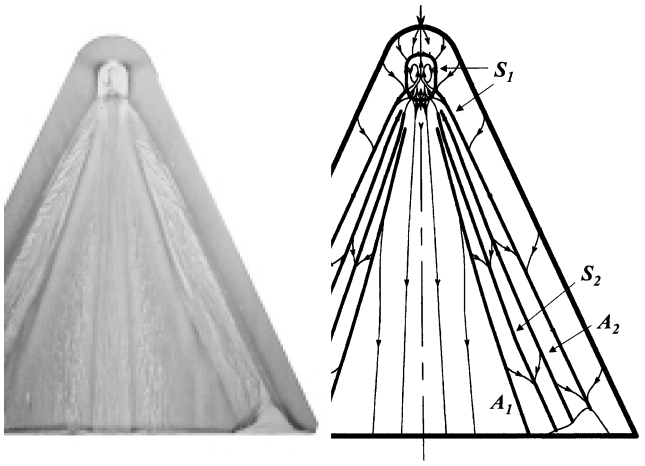

a) $\alpha = 0$ deg

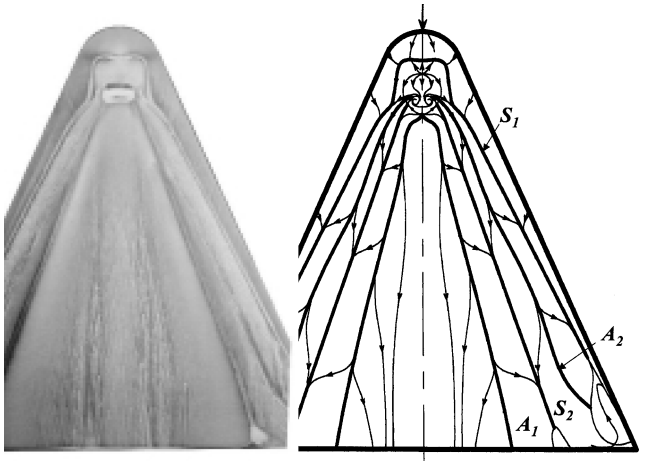

b) $\alpha = 20$ deg

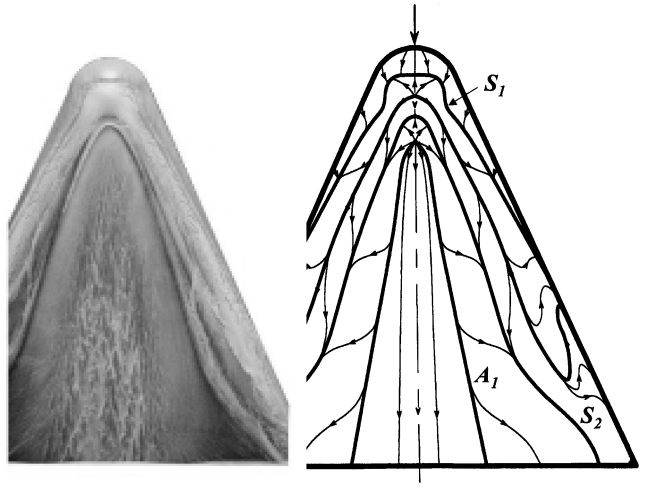

c) $\alpha = 30$ deg

Fig. 14 Effect of α on flow on leeward surface.

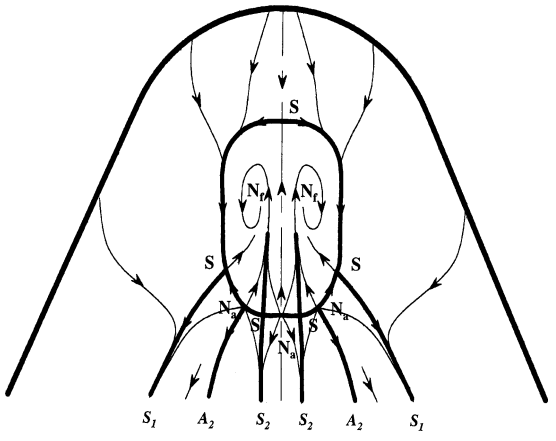

a) $\alpha = 0$ deg

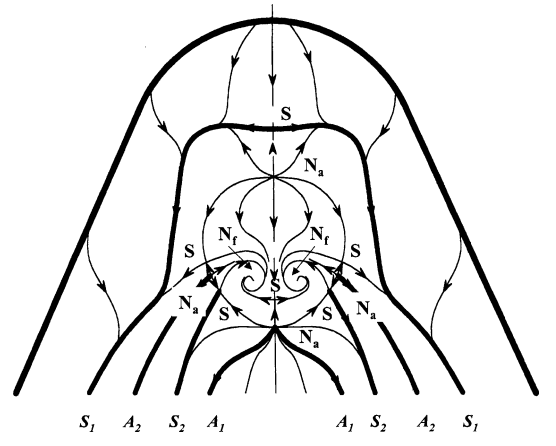

b) $\alpha = 20$ deg

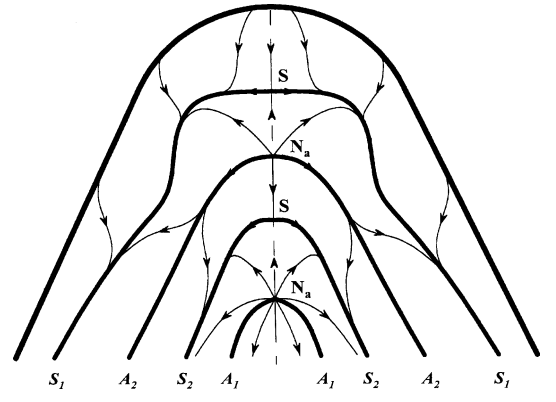

c) $\alpha = 30$ deg

Fig. 15 Conjectured topology of flow on nose.

When α is increased to 5 deg the two counterrotating foci N_f move in downstream direction. The topology of the flow on the model does not bifurcate. A further increase to 10 deg reduces the size of the two foci. In addition, a bifurcation occurs on the centerline; another node and saddle appear on the centerline between the most upstream S and the foci. At $\alpha = 14$ deg, a drastic bifurcation was noted; a second pair of foci shows up downstream of the existing foci. The direction of the new focus pair is opposite that of the already existing focus pair. With increasing α the new foci increase in size and eventually absorb the former pair. The size of the new foci is largest at $\alpha = 20$ deg. Apart from the foci the topology at this angle consists of four nodes and six saddles. The formation of the primary and secondary separation is difficult to determine from this complex topology and is still subject of investigation. The horn-type vortices springing from the foci on the wing surface could be the origin of the primary vortices, at least their direction of rotation correlates. The question is what type of flow is evolving from the more upstream located N_a and S. To obtain more data on the three-dimensional separation processes, for a subsequent study extended surveys of the off-the-surface flow field are planned.

At α beyond 20 deg the foci pair was observed to move in downstream direction and to decrease in size. The pair has vanished at $\alpha = 30$ deg. The flow topology at the latter α is easy to interpret. The topology consists of a twin N_aS combination on the centerline. This is characteristic of a U type of separation. Figure 16 shows the conjectured structure of the off-the-surface flow at this angle of attack.

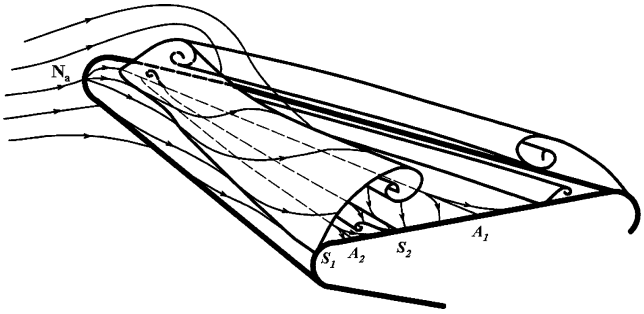

Fig. 16 Conjectured off-the-surface flow at $\alpha = 30$ deg.

The skin-friction line pattern on the apex model shows markings of primary and secondary separation, but no traces of tertiary separation. The latter type of separation may start at a more downstream location. In view of this, a subsequent visualization study will be conducted with a longer version of the apex model.

Discussion

Detailed information has been obtained on the effects of the angle of attack on the topology of the skin-friction line pattern over the apex of a delta wing. This information was generated using a large-scale model of the apex. The leading-edge radius of the apex model is 200 times that of the original delta wing, whereas the apex model is shorter than the latter wing. To have the same flow structure on the apex model and on the apex of the sharp-edged delta wing, theoretically all relevant dimensions should have been scaled up with the same value. In addition, the Reynolds number based on model length should have been the same. The present apex model is too short to satisfy these requirements. A correlation between the flow over this model and that over the front part of the delta wing is therefore not possible. The apex model is a valuable tool to obtain more insight into the flow topology on the nose of a delta wing. This information is hard to obtain with a smaller scale model. For a correlation with the flow over the front part of the delta wing, a more extended apex model would be needed. The dimensions of the wind tunnels available at TUD, however, prevent the testing of such a model.

Conclusions

A study of the flow over a 65-deg delta wing is described. The flow is analyzed qualitatively using topology theory. Because of the small dimensions of the apex, the skin-friction line pattern on this part of the delta wing is poorly resolved. A large-scale apex model was constructed to obtain more information on the apex flow. The flow was visualized at α ranging from zero to 30 deg. The angle of attack is found to have a strong effect on the topology of the skin-friction line pattern at the nose–body transition. The flow pattern shows evidence of primary and secondary separation. No markings are found of a tertiary separation as is believed to exist on the apex of the original delta wing. A longer version of the apex model could show the onset of tertiary separation. Apart from a longer model, for a subsequent study surveys of the outer flow field are recommended in order to obtain more information on the flow separation processes.

References

[1]Mitchell, A. M., Morton, S. A., Huang, X. Z., and Verhaagen, N. G., "NATO RTO AVT Task Group-080 Vortex Breakdown over Slender Delta Wings: Validation and Verification, Conclusions and Recommendations," AIAA Paper 2003-4218, June 2003.

[2]Verhaagen, N. G., and Jobe, C. E., "Topology of the Flow on a 65-deg Delta Wing at Sideslip," AIAA Paper 2002-0095, Jan. 2002.

[3]Lighthill, M. J., "Boundary Layer Theory," *Laminar Boundary Layers*, L. Rosenhead, ed., Oxford Univ. Press, Cambridge, England, U.K., 1963, pp. 46–113.

[4]Délery, J. M., "Robert Legendre and Henri Werlé: Towards the Elucidation of Three-Dimensional Separation," *Annual Review of Fluid Mechanics*, Vol. 33, Jan. 2001, pp. 129–154.

[5]Legendre, R., "Lignes de Courant d'un écoulement continu," *La Recherche Aérospatiale*, No. 105, 1965, pp. 3–9.

[6]Peake, D. J., and Tobak, M., "Three-Dimensional Interactions and Vortical Flows with Emphasis on High Speeds," AGARDograph No. 252, July 1980.

[7]Verhaagen, N. G., and Jobe, C. E., "Effects of Sideslip on the Characteristics of a 65-deg Delta Wing," AIAA Paper 2003-0736, Jan. 2003.

[8]Bakker, P. G., "Bifurcations in Flow Patterns: Some Applications of the Qualitative Theory of Differential Equations in Fluid Dynamics," Kluwer, Dordrecht, The Netherlands, 1991.

[9]Tobak, M., and Peake, D. J., "Topology of Three-Dimensional Separated Flows," *Annual Review of Fluid Mechanics*, Vol. 14, 1982, pp. 61–85.

[10]Hunt, J. C. R., Abell, C. J., Peterka, J. A., and Woo, H., "Kinematic Studies of the Flows Around Free or Surface-Mounted Obstacles-Applying Topology to Flow Visualization," *Journal of Fluid Mechanics*, Vol. 86, Pt. I, 1978, pp. 179–200.

[11]Harvey, J. K., "Some Measurements on a Yawed Slender Delta Wing with Leading Edge Separation," ARC R&M No. 3160, 1961.

[12]Hummel, D., "Zur Umströmung Scharfkantiger Schlanker Deltaflügel bei großen Anstellwinkeln," *Zeitschrift der Flugwissenschaft*, Vol. 15, No. 10, 1967, pp. 376–385.